Contactless measurements of electrical conductivity via the eddy current method

Author: Paula Sierra Varela.
*Facultat de Física, Universitat de Barcelona, Diagonal 645, 08028 Barcelona, Spain.**

Advisor: Cèsar Ferrater Martorell

Abstract: Eddy current method is a non-destructive technique that allows electrical conductivity contactless measurements. This work aims to build and characterize a data-acquisition system that uses this method to measure conductive films' conductivity from a parallel *LC* circuit and a lock-in amplifier. Its functionality is studied by analysing impedance variations of three different samples.

I. INTRODUCTION

Electrical conductivity characterization is important to determine electrical properties of materials. Conventional techniques as four-point-probe method commonly use mechanical contact to measure it [1]. However, thin samples could be damaged or contaminated by applying this procedure. Contactless measurement methods are the solution to this problem, offering effective ways to measure the electrical conductivity without changing the properties of the tested material [2]. One of them is the eddy current technique.

Eddy current method is a fast [3] and non-destructive technique based on the electromagnetic field's interaction with a measuring sample [4, 5]. A coil fed with an alternating current (AC) produces an alternating magnetic field. According to Faraday's law of induction, if a sample is placed close to the coil, the alternating magnetic field induces loop currents in it, which are called eddy currents. Eddy currents cause energy dissipation by the Joule effect. Under quasi-static conditions, the dissipated power per unit mass can be described as [6]:

$$P = \frac{\pi^2 B_p^2 d^2}{6k\rho D} f^2 \tag{1}$$

where B_p is the peak magnetic field; d, ρ and D are the thickness, resistivity, and density of the sample, respectively; k is a constant; and f is the frequency. From Eq. (1), one can see that eddy currents depend, among other parameters, on the electrical conductivity of the sample. These currents produce, as stated by Lenz's law, a magnetic field that interacts with the starting alternating magnetic field of the coil. Consequently, the inductance of the coil changes, and so does the impedance. These impedance variations can be easily measured and are the basis of the eddy current method.

Coil's impedance behaviour is given by Eq. (2)

$$Z_L = R_L + iL\omega \tag{2}$$

where L and R_L are the inductance and the resistance of the coil, respectively. For an ideal coil, its self-resistance is negligible, and a linear behaviour is shown for all the frequency range. However, in a real coil, R_L becomes more relevant as frequency decreases, as can be seen in Fig. (1).

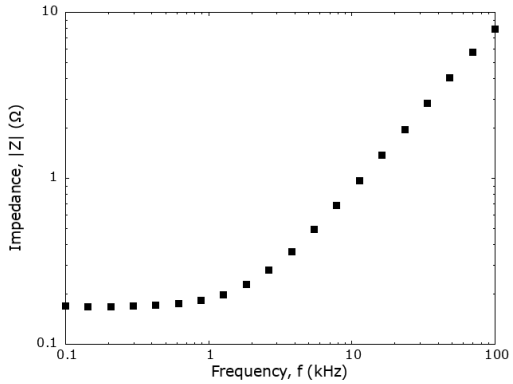

FIG. 1: Coil's impedance modulus vs. frequency. Two regions can be observed. At $f < 1$ kHz, impedance's real term is dominant, while at values of $f > 1$ kHz, impedance modulus shows a linear behaviour. R_L and L can be obtained from these frequency ranges, respectively.

To avoid this problem, the operating range of frequencies used is of the order of kHz. It is important to note that the operating frequency (f) is not the same as the radial frequency (ω), where $\omega = 2\pi f$. In order to improve the measurement sensitivity, a capacitor is connected in parallel to the sensing coil. The anti-resonant circuit behaviour without any sample is shown in Fig. (2).

Impedance variations caused by eddy currents can be analysed via different methodologies. On the one hand, as these impedance changes translate into a displacement of the anti-resonant peak, one can compare the resulting anti-resonant frequencies' positions and their corresponding impedance values. On the other hand, equivalent impedance behaviour for a parallel *LC* circuit is described by

$$(Z_{RLC})_{parallel} = \frac{Z_C \cdot Z_{RL}}{Z_C + Z_{RL}} = \frac{R_L + iL\omega}{1 - \omega^2 LC + i\omega R_L C} = \frac{R_L + i\left(-\omega C R_L^2 + L\omega(1 - LC\omega^2)\right)}{(1 - \omega^2 LC)^2 + (\omega R_L C)^2} \tag{3}$$

where L and R_L are again the inductance and the resistance of the coil, and C is the capacitance of the circuit's capacitor.

* Electronic address: psierrva26@alumnes.ub.edu

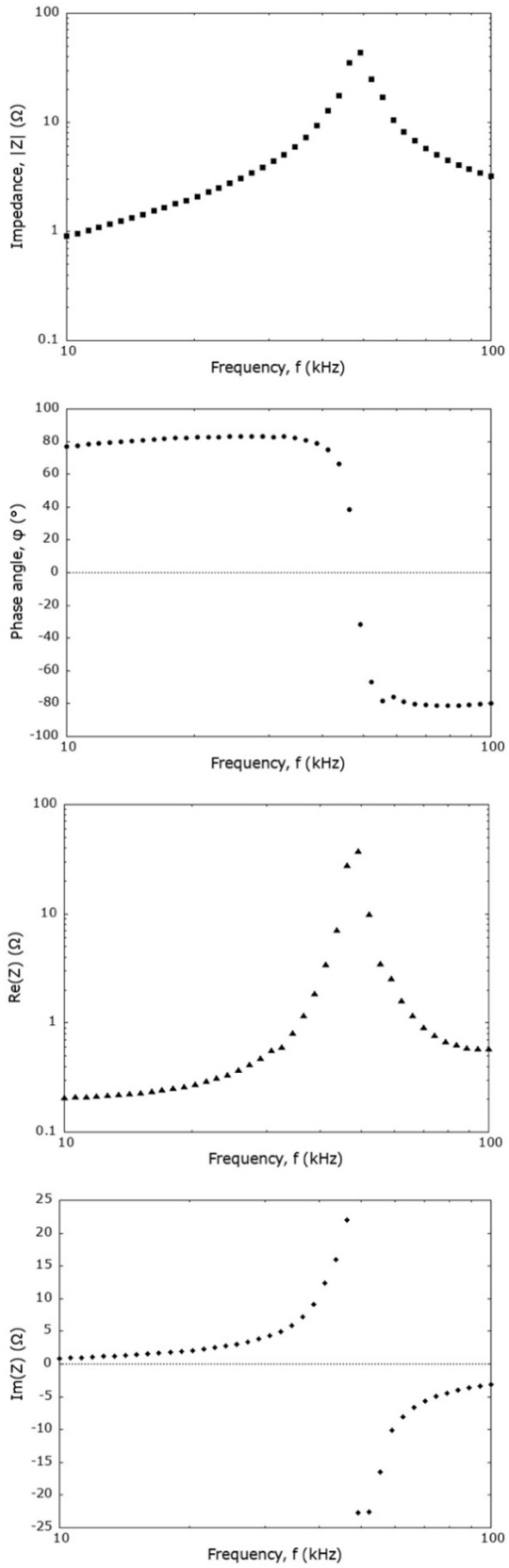

FIG. 2: From top to bottom: impedance modulus, phase angle, impedance's real part, and impedance's imaginary part vs. frequency for the anti-resonant circuit without any sample.

As $|iL\omega| \gg R_L$

$$Z_C \cdot Z_{RL} \simeq \frac{1}{i\omega C} \cdot i\omega L = \frac{L}{C} \tag{4}$$

Moreover, under anti-resonance condition

$$Z_C + Z_{RL} = R_L \tag{5}$$

Combining (4) and (5), Eq. (3) can be rewritten as

$$(Z_{RLC})_{0\ parallel} = \frac{L}{CR_L} \tag{6}$$

that gives us the anti-resonance impedance value for the parallel resonant frequency $\omega_0 = \sqrt{(L - R_L^2 C)/L^2 C}$ [7]. From Eq. (6), one can easily see that a change on the anti-resonance impedance implies an alteration of the parameters L, C and/or R_L. In this way, our study can be done from analysing this parameters' deviation.

When studying thin samples, it is convenient to measure their sheet resistance rather than their specific conductivity. For a homogeneous rectangular parallelepiped sample, its resistance can be expressed as [8]:

$$R = \rho \frac{l}{D \cdot w} = R_S \frac{l}{w} \tag{7}$$

where ρ and D are again the resistivity and thickness of the sample, and l and w are its length and width, respectively. R_S is the sheet resistance. Its interest lies in the fact that, given a uniform thickness, it is an excellent parameter to characterize conductivity since the relation ρ/D is constant throughout the sample [8].

This work aims to build and characterize a system that allows contactless conductivity measurements on thin conductive samples based on the eddy current method operation for different conductive materials.

II. EXPERIMENTAL

The experimental setup is shown in Fig. (3). The sensing coil $(L = (1{,}28 \pm 0.01) \times 10^{-5}\ H; R_L = 0.168 \pm 0.001\ \Omega)$ is 1,4 cm in diameter and is winded using copper wire. The capacitor C is 820 nF.

A lock-in amplifier (AMETEK Model 7265 DSP) is used to measure the coil's impedance, its real and imaginary parts, and the phase. The measuring frequency range enabled is 0,001 Hz to 250 kHz [9].

A lock-in amplifier is a measurement system and a signal processor that efficiently separates signal from noise. The measuring signal is applied to the amplifier through a coaxial connector BNC, leading it to act like a voltmeter or an ammeter, depending on the input connectors selected. In order to measure this periodical signal, the lock-in needs an auxiliary reference signal of the same period. It can be generated by an external or an internal source, and it is used

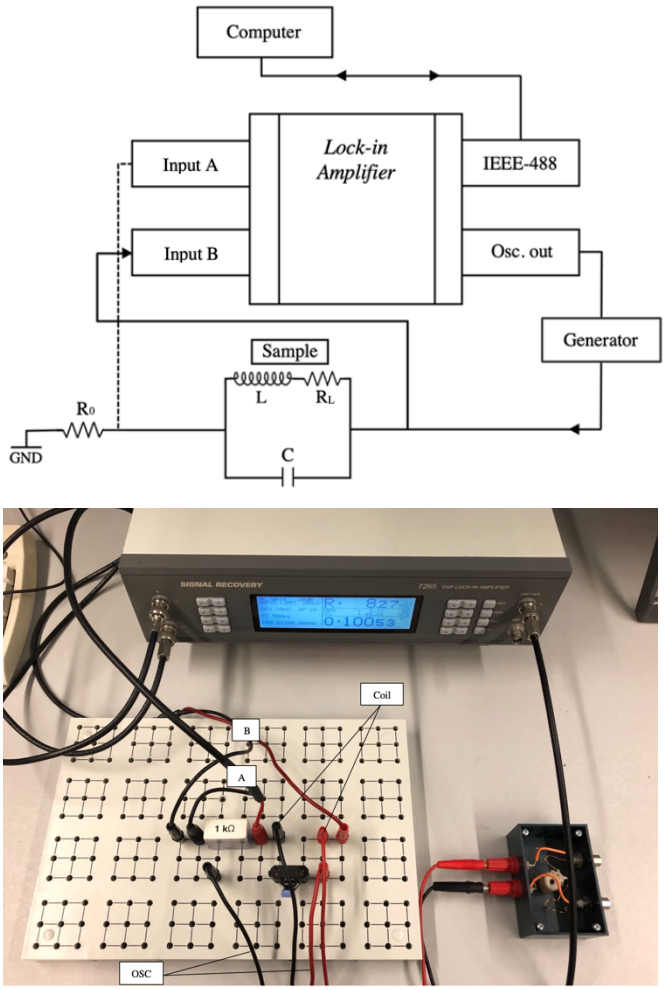

FIG. 3: Block diagram and image of the experimental setup.

by a PLL (phase-locked-loop) dispositive to produce an internal sinusoidal signal of the same frequency. Finally, the measuring and the reference signals are multiplied, and two independent low-pass filters return a time average. A digital voltmeter measures the continuous component of the voltage and presents the result on the monitor.

In our measurements, lock-in amplifier operation and data acquisition were controlled by a PC via an IEEE 488/USB connection by a computer program written in an Excel environment[1]. Voltage-type input connectors were used, and no initial frequency rejection filters were applied. The amplifying factor (sensitivity) was set into automatic mode to achieve the maximum possible value without producing input saturation. On the other hand, low-pass filter parameters were fixed on 500 ms for the time constant and 12 dB/octave for the slope.

III. RESULTS AND DISCUSSION

In this work, three different conductive samples have been studied. To start with, this study explores the impedance behaviour of two limiting cases. The first case is that of a very high sheet resistance and corresponds to the system without any sample, shown in Fig. (2). In the second case, an aluminium block sample with a sheet resistance close to zero is analysed. These two limiting cases are used to study the system's functionality via the impedance variations of two thin samples, PASCO's PK-9025 conductive paper and a transparent conducting oxide (TCO). The study develops these present differences by means of a graphical fitting computed using Eq. (3). The resulting parameters for the limiting cases and the samples under test are specified in Table I, and the impedance variations from the system behaviour without any sample are shown in Fig. (4).

TABLE I: Impedance fitting parameters and anti-resonant frequency of the two limiting cases (anti-resonant circuit without any sample ($R_S \gg 0$) and aluminium block sample ($R_S \approx 0$)) and the samples under test.

	L (H)	C (nF)	R (Ω)	ω_0 (10^5 rad/s)
No sample ($R_S \gg 0$)	$1.32 \cdot 10^{-5}$	827	0.33	3.02 ± 0.01
Aluminium block ($R_S \approx 0$)	$1.17 \cdot 10^{-5}$	827	0.36	3.20 ± 0.01
Conductive paper	$1.30 \cdot 10^{-5}$	827	0.33	3.04 ± 0.02
TCO	$1.37 \cdot 10^{-5}$	817	0.33	2.98 ± 0.02

It is important to note that the fitting is made to adjust exclusively to the region close to the anti-resonant frequency. The data series' observed discontinuities are an instrumental effect.

As would be expected, the aluminium block sample corresponding to the $R_S \approx 0$ limiting case shows the most significant variations on both the fitting parameters and the anti-resonant frequency. We can observe that both L and R have changed from the initial fitting values of the system without any sample, while the value for C continues to be the same.

The impedance behaviour of the conductive paper sample lays in the intermediate region between the two limiting cases. In this case, L has slightly decreased in relation to the initial fitting value, while R and C remain constant.

Finally, the TCO sample behaves opposite to both the limiting case of the aluminium block and the conductive paper. Now, L has increased, while C has decreased. R remains constant. This opposite behaviour regarding the previous samples might indicate that this sample behaves as a dielectric since transparent conductive materials are degenerate semiconductors. This leads to an alteration of C because of the dielectric contribution.

[1] Excel ® *Lock-in* created by Dr. José Miguel Asensi López.

A. Aluminium block B. Conductive paper C. TCO

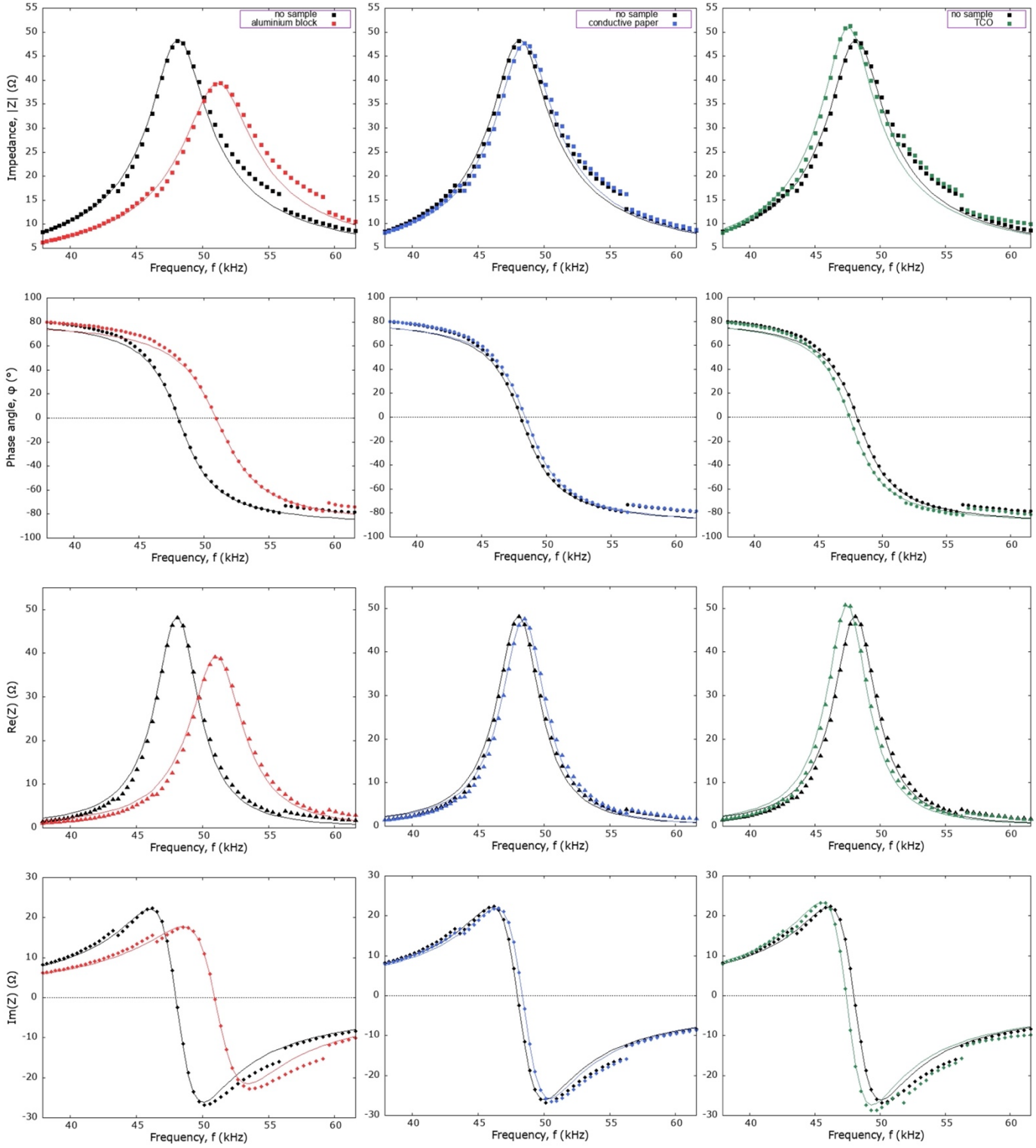

FIG. 4: Each column represents one of the samples under test. From top to bottom: impedance modulus, phase angle, impedance's real part, and impedance's imaginary part vs. frequency for the three samples, respectively. Points represent the acquired data series, and lines correspond to the fitting. Each plot includes the no-sample case behaviour (in black).

Fig. (5) shows a comparison of the results obtained for the three samples and the circuit ones.

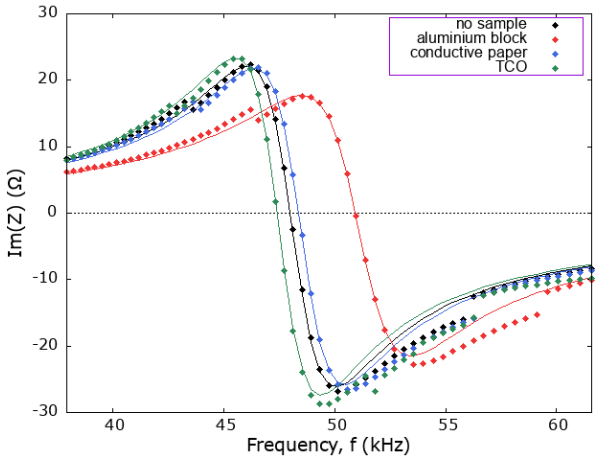

FIG. 5: Impedance's imaginary part vs. frequency for the two limiting cases and the samples under test.

It is noticeable that, for more conductive samples, the difference between their anti-resonant frequency and the no-sample one increases. This also holds for the relationship between the fitting parameters for each case. The aluminium block anti-resonance peak tends to decrease while moving toward the right. As would be expected, the conductive paper impedance curve lays between the two limiting cases. However, TCO's one shifts towards the left, remaining outside these mentioned limits.

IV. CONCLUSIONS

- The study enables contactless and non-destructive measurements using the eddy current method. Impedance dependence with frequency shows distinct differences for the different sheet resistances, both on the anti-resonant frequencies and the parameters for parallel impedance fitting.
- Results for the conductive paper sample show that its parallel impedance fitting parameters and anti-resonant frequency lay between the two limiting cases of sheet resistance, as expected. However, the impedance behaviour for the TCO sample lays outside the expected ranges for sheet resistance. This might be due to a contribution of capacitance because of its dielectric behaviour.
- In order to obtain the sheet resistance of the studied samples, modelling of the currents' distribution and the conductive behaviour of the sample, incorporating it into the equivalent circuit, would be necessary. On the other hand, an AC bridge setup would be convenient to increase the measurement sensitivity.

Acknowledgments

I would like to thank my advisor Dr. Cèsar Ferrater Martorell for his help, availability, and counselling during these months, as well as Dr. José Miguel Asensi López for providing the program used to control the lock-in amplifier operation and data acquisition.

I would also like to thank my family and friends for their support and care.

[1] N. Bowler and Y. Huang, «Electrical conductivity measurement of metal plates using broadband eddy-current and four-point methods,» *Measurement Science and Technology,* vol. 16, pp. 2193-2201, 2005.

[2] J. García-Martín, J. Gómez-Gil and E. Vázquez-Sánchez, «Non-destructive techniques based on eddy current testing,» *Sensors,* vol. 11, no. 3, pp. 2525-2565, 2011.

[3] W. Li, Y. Ye, K. Zhang and Z. Feng, «A thickness measurement system for metal films based on eddy-current method with phase detection,» *IEEE Transactions on Industrial Electronics,* vol. 64, no. 5, pp. 3940-3949, 2017.

[4] D. F. He, K. Zhang and J. Tang, «A contacless method to measure the electrical conductivity,» in *IEEE 3rd International conference on control science and systems engineering*, 2017.

[5] S. F. Dmitriev, V. N. Malikov, A. V. Ishkov, A. O. Katasonov and A. M. Sagalakov, «Application of an eddy-current method to measure electrical conductivity of thin films,» in *IOP Conf. Series: Materials Science and Engineering 441*, 2018.

[6] F. Fiorillo, Measurement and Characterization of Magnetic Materials, Elsevier Academic Press, 2004, p. 31.

[7] B. Esteban, J. R. Riba, G. Baquero and C. Ferrater, «An eddy-current-based sensor for preventing knots in metallic wire drawing processes,» *Nondestructive Testing and Evaluation,* vol. 26, no. 2, pp. 169-180, 2011.

[8] A. Santacreu, «Sheet resistance and Van Der Pauw method,» Treball de Fi de Grau. Universitat de Barcelona, 2017.

[9] AMETEK, «Model 7265 DSP Lock-in Amplifier. Instruction Manual.,» 2002. [Online]. Available: https://groups.spa.umn.edu/zudovlab/manuals/measurement/SR7265m.pdf. [Accessed November 2022].